Journal of Zhejiang University-SCIENCE A (Applied Physics & Engineering) 2023 24(6):543-556
www.jzus.zju.edu.cn; www.springer.com/journal/11582
E-mail: jzus_a@zju.edu.cn

Research Article

https://doi.org/10.1631/jzus.A2200405

Compressive properties of a novel slurry-infiltrated fiber concrete reinforced with arc-shaped steel fibers

Hedong LI[1], Yabiao LI[1], Yunfeng PAN[1]✉, P.L. NG[2,3]✉, Christopher K.Y. LEUNG[4], Xin ZHAO[5]

[1]*School of Civil Engineering and Architecture, Zhejiang Sci-Tech University, Hangzhou 310018, China*
[2]*Department of Civil Engineering, The University of Hong Kong, Hong Kong 999077, China*
[3]*Faculty of Civil Engineering, Vilnius Gediminas Technical University, Vilnius LT-10223, Lithuania*
[4]*Department of Civil and Environmental Engineering, The Hong Kong University of Science and Technology, Hong Kong 999077, China*
[5]*School of Civil Engineering and Architecture, Zhejiang University of Science and Technology, Hangzhou 310023, China*

Abstract: Slurry-infiltrated fiber concrete (SIFCON) is a sort of strain hardening cement-based composite material, typically made with 5%–20% steel fibers. This study focused on a novel type of SIFCON in which hooked-end steel fibers were replaced by arc-shaped steel fibers. The quasi-static compressive properties of the SIFCON were first measured. Test results suggested that using arc-shaped steel fibers in lieu of hooked-end steel fibers increased the quasi-static compressive strength by 47.1% and the strain at peak stress by 56.3%. We attribute these improvements to new crack-resisting mechanisms, namely "fiber cross-lock", "dual bridging", and "confinement loops", when the arc-shaped steel fibers are introduced into SIFCON. As high impact resistance is a special property of SIFCON that is of practical significance, the dynamic compressive properties of arc-shaped steel fiber SIFCON were studied by using an 80-mm-diameter split Hopkinson pressure bar (SHPB). The results showed that the dynamic compressive strength, dynamic increase factor (DIF), and dynamic toughness of SIFCON all increased with the strain rate. The SIFCON incorporating arc-shaped steel fibers proved to have significant advantages in structural applications requiring high impact resistance.

Key words: Slurry-infiltrated fiber concrete (SIFCON); Arc-shaped steel fiber; Quasi-static compressive properties; Spilt Hopkinson pressure bar (SHPB); Dynamic compressive properties

1 Introduction

Slurry-infiltrated fiber concrete (SIFCON) is an ultra-high performance cementitious composite with significant strain-hardening properties first developed in the early 1980s (Kar, 1984). SIFCON contains 5%–20% steel fibers due to a casting process that differs from that of traditional steel fiber reinforced concrete (SFRC) which contains about 2% steel fibers. SIFCON is created by preplacing steel fibers in the mold to form a fiber network that will be infiltrated with cementitious paste or mortar. The tensile and compressive properties of SIFCON are superior to those of conventional concrete, with a tensile strength of 35 MPa and a compressive strength of 210 MPa (Homrich and Naaman, 1987; Naaman et al., 1992). It also has excellent toughness characteristics and outstanding ductility and energy absorption properties (Lankard, 1985; Naaman et al., 1992; Reinhardt and Naaman, 1992). The desirable mechanical properties of SIFCON render it a favourable material for pavement rehabilitation, structural strengthening, and seismic or blast resistant structures (Lankard, 1984; Elnono et al., 2009).

The mechanical performance of SIFCON is determined mainly by the fiber type and volume fraction, as well as the performance of the brittle matrix (Naaman et al., 1992; Drdlová et al., 2016; Soylu and Bingöl, 2019; Khamees et al., 2020; Renuka and Rajasekhar, 2021). The cement paste volume has a considerable influence on the performance of high-performance concrete (Piasta and Zarzycki, 2017). A large paste volume decreases the compressive strength

✉ Yunfeng PAN, yfpan@zstu.edu.cn
P.L. NG, irdngpl@gmail.com
Hedong LI, https://orcid.org/0000-0002-0911-1976

Received Aug. 21, 2022; Revision accepted Nov. 28, 2022;
Crosschecked Mar. 23, 2023; Online first May 17, 2023

of the concrete (Kolias and Georgiou, 2005; Chu, 2019). Some recent studies (Chu, 2021; Kong et al., 2022) have reported a new type of fiber reinforced concrete called infilled cementitious composite (ICC). It has a minimal paste volume while ensuring high fresh and hardened performance. In addition, the function of the steel fibers is derived mainly from the bond that exists between the fibers and the matrix, the frictional resistance that has to be overcome during the fiber pull-out process, and the mechanical interlocking force generated by "fiber interlock", especially when the fiber volume content is high (Homrich and Naaman, 1987). The pull-out performance of steel fiber from the cementitious matrix is significantly affected by the fiber shape, fiber end geometry, and matrix strength. In general, the bonding performance of hooked-end steel fibers is often superior to that of straight fibers (Tuyan and Yazıcı, 2012). Homrich and Naaman (1987) found that the compressive strength of SIFCON reinforced with hooked-end steel fibers was higher than that of SIFCON reinforced with crimped steel fibers. Ipek and Aksu (2019) found that the flexure strength of a SIFCON beam could reach 44 MPa when it was filled with hooked-end steel fibers. The hooked-end steel fibers significantly improve the compressive strength, ductility, and toughness of fiber reinforced concrete (Wu et al., 2018; Kim et al., 2020; Shi et al., 2020; Naji et al., 2021). Therefore, better mechanical properties might be obtained by using fibers that have a stronger bond with the cementitious matrix. In view of the above, this study focused on arc-shaped steel fibers, which would provide a significantly higher bond strength than hooked-end steel fibers and conventional straight steel fibers (Won et al., 2015a; Kim et al., 2021). Won et al. (2015b) studied the flexural properties of cementitious composites reinforced with arch-type steel fibers (similar to arc-shaped steel fibers). They found that arch-type steel fiber reinforced cementitious composites had higher flexural strength than cementitious composites with the same volume content of hooked-end steel fibers. Hence, we hypothesized that replacing traditional steel fibers with arc-shaped steel fibers would have great potential to enhance the mechanical performance of SIFCON.

The high impact resistance of SIFCON is one of its beneficial properties in practical applications. Previous investigations of the dynamic properties of SIFCON have been conducted mainly using drop-hammer impact tests (Rao et al., 2010; Elavarasi and Saravana Raja Mohan, 2018; Abirami et al., 2019), projectile penetration tests (Gulkan and Korucu, 2011; Korucu and Gulkan, 2011), and contact detonation tests (Chun et al., 2013; Drdlová et al., 2018a, 2018b; Morishima et al., 2020). Elavarasi and Saravana Raja Mohan (2018) studied the response of reinforced and unreinforced SIFCON thin slabs to low-velocity impact through drop-hammer impact experiments, and compared them with plain cement concrete (PCC) and reinforced cement concrete (RCC) slabs. The results showed that SIFCON slabs had a significantly higher energy absorption capability than PCC and RCC slabs. Rao et al. (2010) and Abirami et al. (2019) suggested that each steel fiber in the SIFCON slab acted as a miniature energy-absorber. Furthermore, after the initial crack appeared, stress was transferred back to the matrix by fibers crossing the crack, resulting in the formation of multiple cracks and hence an increased energy absorption. Additionally, the high crack bridging stresses significantly decreased the stress intensity at the crack tip and delayed crack propagation in slab specimens.

In general, experimental studies of the dynamic performance of concrete are divided into three distinct categories: low strain rates ($1–10^2$ s^{-1}), high strain rates ($10^2–10^4$ s^{-1}), and ultra-high strain rates ($10^4–10^6$ s^{-1}) (Bischoff and Perry, 1991). A drop hammer impact test is applicable only in the low strain rate range. However, the high strain rate range is critical for a variety of practical applications, such as explosion-resistant military structures and safe vaults (Schneider, 1992) and the lining of tunnels excavated by means of the drill-and-blast method, whereby a high strain rate is generated by blasting (Persson et al., 1993). However, studies on the compression properties of SIFCON at high strain rates are lacking. To test the dynamic performance of materials at high strain rates, the split Hopkinson pressure bar (SHPB) can be used (Kolsky, 1949; Ogawa, 1984). Though impact testing of conventional mortar and concrete has been performed with SHPBs (Ross et al., 1989; Su et al., 2014), they have not been used to test SIFCON.

Based on the above discussion, our research study consisted of two parts. Firstly, to examine the positive influence of arc-shaped steel fibers on the mechanical performance of SIFCON, the quasi-static compressive

performance of SIFCON made with hooked-end steel fibers and arc-shaped steel fibers was compared experimentally. Secondly, the dynamic compressive properties of the arc-shaped steel fiber SIFCON were examined with SHPB to study the impact performance in various strain rate regimes. The effect of different strain rates on the failure patterns, stress-strain curves, compressive strength, and dynamic toughness of the cementitious matrix phase (brittle matrix) and the SIFCON are also presented and discussed in this paper.

2 Experimental details

2.1 Experimental materials and mixture proportions

Two types of steel fibers were used in this experiment, namely ordinary hooked-end steel fibers and arc-shaped steel fibers (Fig. 1). The overall length of the hooked-end steel fibers was 30 mm, with a hook of about 4 mm in length at each end. Table 1 lists their geometrical and physical properties. Each arc-shaped steel fiber consisted of a circular arc segment and two end-anchored segments; it represented a bent version of the hooked-end steel fiber described above. Referring to the terminology of an arch structure, the "span" of the arc-shaped steel fiber was about 18 mm and the "rise" about 11 mm. Therefore, the two types of steel fibers differed in shape, but had the same length and performance parameters.

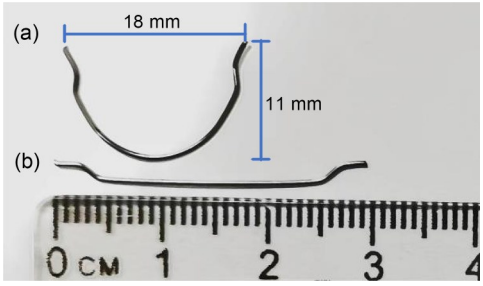

Fig. 1 Steel fibers used: (a) arc-shaped steel fiber; (b) hooked-end steel fiber

Table 1 Performance parameters of steel fibers

Type	Length, L (mm)	Diameter, d (mm)	Aspect ratio, L/d	Tensile strength (MPa)	Density (kg/m^3)
Hooked-end	30.0	0.50	60	1100	7800

In this study, Chinese standard Grade 52.5 P.II type Portland cement was used. As additional mineral admixtures, fly ash and silica fume were used. The chemical composition of the fly ash is listed in Table 2. Fine sand with a particle size of less than 0.35 mm at its maximum was used as the fine aggregate. A polycarboxylate superplasticizer (SP) with a water reduction rate greater than 35% was used. The mixing water was laboratory tap water. Table 3 presents the mixture proportions of the cementitious matrix and the volume fractions of steel fiber.

Table 2 Chemical composition of fly ash

Material	Chemical composition (%, mass fraction)							
	Al_2O_3	SiO_2	SO_3	CaO	K_2O	TiO_2	Fe_2O_3	MgO
Fly ash	40.53	40.74	1.20	7.05	1.23	2.09	6.10	1.07

2.2 Specimen preparation

To prepare the SIFCON specimens, each mold was first filled with steel fibers to form a fiber network. Then it was weighed to obtain the total mass of steel fibers, and the actual steel fiber volume fraction was obtained by calculation. The calculated volume fractions of hooked-end steel fiber and arc-shaped steel fiber were 12.8% and 12.4%, respectively. The cementitious mortar was batched and mixed thoroughly in a mortar mixer, and then infiltrated into the fiber network with micro-vibration on a vibrating table. At the SP dosage adopted, the flowability of the cementitious mortar was sufficient to penetrate through the dense fiber network. The mini slump flow and V-funnel test mentioned by Manolia et al. (2018) were used to determine the flowability of the cementitious mortar. The spread diameter of mini slump flow was 380 mm and

Table 3 Mixture proportions of the cementitious matrix and the volume fractions of steel fiber

Sample No.	w/b	CPV (%)	V_f (%)	Mixture proportion (kg/m^3)					
				Cement	Fly ash	Silica fume	Sand	Water	SP
Brittle matrix	0.30	42.9	0.0	593	274	46	913	274	4.9
H-SIFCON	0.30	30.1	12.8	593	274	46	913	274	4.9
A-SIFCON	0.30	30.5	12.4	593	274	46	913	274	4.9

H-SIFCON stands for hooked-end fiber SIFCON; A-SIFCON stands for arc-shaped fiber SIFCON; w/b (water to binder ratio) is equal to water/(cement+fly ash+silica fume); CPV represents the volume fraction of cementitious paste; V_f represents the volume fraction of steel fiber

the flow time of the V-funnel test was 8.0 s. It was then necessary to cure each specimen for 24 h in the laboratory before the mold could be removed. The specimens were continuously cured in a standard curing chamber (regulated at a temperature of (20±3) °C and relative humidity of ≥95%) for 28 d before testing.

Cylindrical PVC tubes of different diameters were used as the molds for the test specimens. For the quasi-static compression test, specimens of two different sizes were prepared. Cylinders of Φ100 mm×200 mm in height were used for the quasi-static testing of H-SIFCON (i.e., SIFCON incorporating hooked-end steel fibers) and A-SIFCON (i.e., SIFCON incorporating arc-shaped steel fibers). For the dynamic compression tests of brittle matrix and A-SIFCON, cylindrical specimens of Φ68 mm×34 mm in height were adopted. A total of 24 dynamic compression specimens were prepared. For each material, two groups were prepared for testing under quasi-static loading and three impact strain rates. There were four groups of brittle matrix and A-SIFCON specimens, with three specimens in each group. All specimens were finished by casting at one time. For each group, three Φ68 mm×136 mm-high cylinders were first prepared and, after curing for 28 d, the dynamic compression specimens were cut into Φ68 mm×34 mm-high cylinders. The two end surfaces of these cylinders were polished using a high-precision surface grinder. After that, the parallelism of both ends of each processed specimen was tested using a micrometer. It was necessary to ensure that the roughness of the surfaces of the specimens was less than 0.05 mm. The appearance of an A-SIFCON dynamic compression test specimen is shown in Fig. 2.

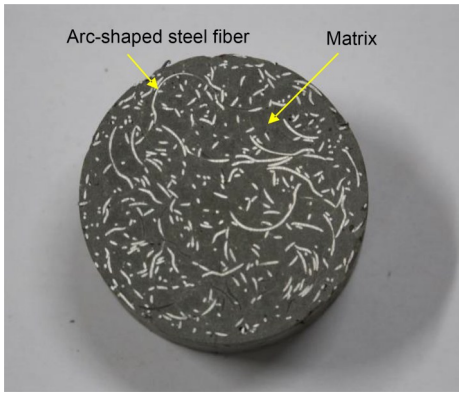

Fig. 2 A-SIFCON dynamic compression test specimen

2.3 Quasi-static tests

A 1000-t electro-hydraulic servo universal testing system was used for the quasi-static compression test. Each cylindrical specimen was loaded at a rate of 0.5 mm/min under displacement control. The corresponding quasi-static compressive strain rate was 4.17×10^{-5} s^{-1} (Kim and Choi, 2006).

2.4 Dynamic tests

Fig. 3 shows the SHPB test system with an 80-mm-diameter pressure bar for dynamic compression testing. The lengths of incident, transmitted, strike, and absorbed bars were respectively 4000, 2500, 800, and 1500 mm. The pressure bar was made of 35CrMnSiA steel with a yield strength higher than 1.2 GPa, and was supported on a ball bearing base with a total length of 12 m. Two BX120-5AA strain gauges (each 5 mm long and 3 mm wide) were symmetrically attached to the middle position of the transmitted and incident bars. The strain gauges were connected to hyperdynamic strain gauges. A half-bridge was used to connect the strain gauges, which were attached a moderate distance from the sample to ensure that the incident wave and reflected wave did not interfere with each other. We assumed that the waveform of a one-dimensional stress wave would not distort during

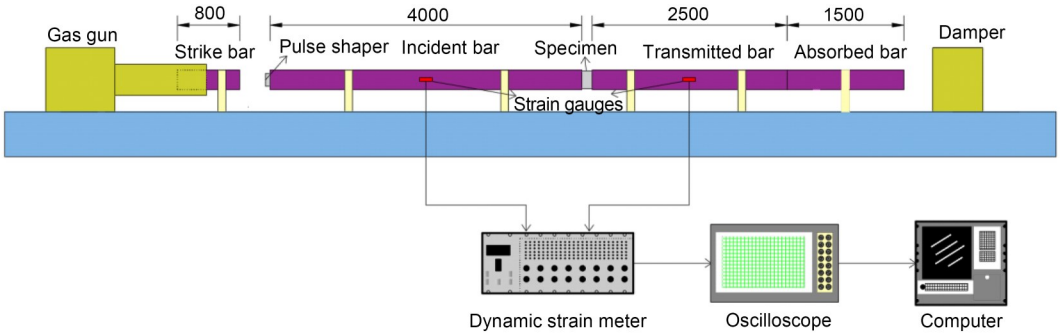

Fig. 3 Split Hopkinson pressure bar (SHPB) test setup (unit: mm)

propagation along the SHPB. Therefore, the stress waveform measured by strain gauges at any position along the bar would be consistent with that at the surface of the sample. The sample was clamped between the transmitted and incident bars during the test, and some vacuum grease was added to the surface of the sample to reduce any possible end friction effect.

The strike bar was driven by nitrogen and launched to collide with the incident bar, generating incident stress waves. When the incident wave reached the interface of the sample, reflection and transmission stress waves would be generated. The hyperdynamic strain gauges attached to the bar were used to obtain the wave signals from the incident, reflected, and transmitted pulses. The strain signals were amplified by the bridge amplifiers connected to the data acquisition system and digitized by the oscilloscope. The collected data were then processed to derive the dynamic stress (σ), strain (ε), and strain rate ($\dot{\varepsilon}$), as per the following formulae:

$$\sigma=\frac{A}{A_0}E_0\varepsilon_t,\ \varepsilon=\frac{2C_0}{L_0}\int_0^t\varepsilon_r\,\mathrm{d}t,\ \dot{\varepsilon}=\frac{2C_0}{L_0}\varepsilon_r, \tag{1}$$

where A and A_0 are the cross-sectional areas of the bar and the specimen, respectively, C_0 and E_0 are the elastic wave speed and the elastic modulus of the bar, respectively, L_0 is the length of the specimen, and ε_t and ε_r are the strains of the transmitted pulse and reflected pulse, respectively.

The incident stress waveform could be controlled by adjusting the air pressure, such that the strain rate of the material could be altered accordingly. Three sets of air pressures (0.450, 0.738, and 1.000 MPa) were applied for each material. The corresponding strain rates ranged from 22.7 to 190.4 s^{-1}, which span from low strain rate to high strain rate regimes.

3 Results and discussion

3.1 Quasi-static compressive properties

Fig. 4 shows the quasi-static compressive stress-strain curves of H-SIFCON and A-SIFCON specimens. The compressive strength and strain at peak stress of the A-SIFCON (169.6 MPa and 5.0%, respectively) were much greater than those of the H-SIFCON (115.3 MPa and 3.2%). To put it another way, at peak stress of SIFCON the compressive strength was increased by 47.1% and the strain by 56.3% by replacing hooked-end steel fibers with arc-shaped steel fibers and keeping the matrix strength unchanged. Fig. 5 shows a comparison of quasi-static compressive stress-strain curves between the A-SIFCON and other H-SIFCON from the literature (Homrich and Naaman, 1987; Kim and Choi, 2006; Kim et al., 2020). The quasi-static compression properties of A-SIFCON outperform those of H-SIFCON reported elsewhere.

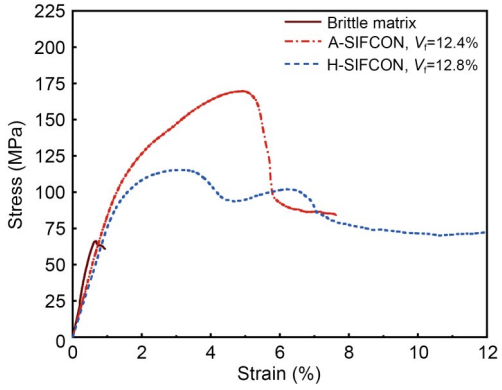

Fig. 4 Quasi-static compressive stress-strain curves of SIFCON incorporating different steel fibers

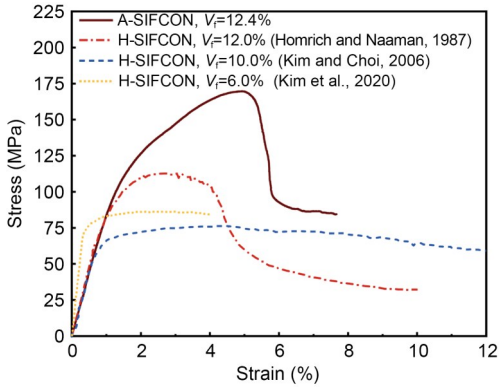

Fig. 5 Comparison of quasi-static compressive stress-strain curves between A-SIFCON and other H-SIFCONs

Fig. 6 depicts the typical failure modes of SIFCON under a quasi-static load. The compression failure mode was observed for H-SIFCON specimens, whereas the shear failure mode was found for A-SIFCON specimens. During the test, small transverse cracks were generated and developed with the increase of load near the middle part of the H-SIFCON specimens. A large amount of matrix detached and steel fibers in the lower part of the specimens were pulled out, while the other parts remained intact. The specimens exhibited large compressive deformation, and obvious

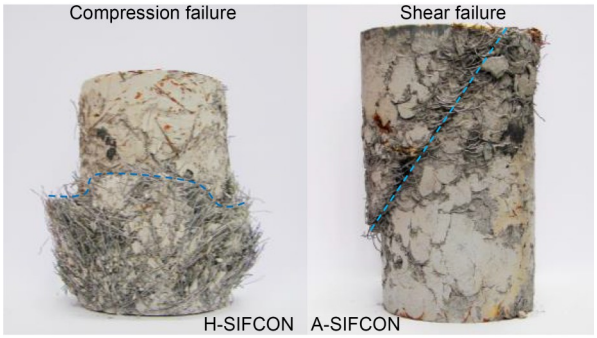

Fig. 6 Failure modes of SIFCON under quasi-static compressive tests

compression cracks appeared in the middle region. These results are consistent with those of Kim and Choi (2006). During the testing of A-SIFCON specimens the matrix and the arc-shaped steel fibers deformed integrally at first. As the load continued to increase, a small number of micro-cracks appeared in the diagonal plane of the specimens. The bond between the fiber and matrix was then weakened, resulting in the spalling of some matrix. When the load further increased, the specimens slipped along a diagonal plane and an obvious shear cracking zone was visible, eventually leading to failure (Fig. 6).

3.2 New mechanisms associated with arc-shaped steel fibers

The "fiber interlock" effect between hooked-end steel fibers was considered to be the main reason for the excellent mechanical properties of SIFCON (Homrich and Naaman, 1987). However, the preparation of SIFCON using arc-shaped steel fibers could give rise to a number of new crack-resisting mechanisms. Compared with hooked-end steel fibers, arc-shaped steel fibers could better enhance the mechanical properties of SIFCON in the following ways:

(1) The interlocking force produced by the "cross-lock" of arc-shaped steel fibers is theoretically much greater than that generated by the "fiber interlock" between hooked-end steel fibers, rendering it difficult for the arc-shaped steel fibers to be pulled out from the SIFCON. Moreover, the "fiber cross-lock" allows the load to be transmitted further when subjected to compression force, thereby mobilizing a larger volume of SIFCON to participate in resisting the external force.

(2) It is possible that the arc-shaped steel fibers realize "dual bridging" over the crack surface, thereby enhancing the crack bridging efficiency of arc-shaped steel fibers compared with hooked-end steel fibers, which allow only "single bridging" over the crack surface.

(3) The arc-shaped steel fibers can effectively confine a crack opening by creating "confinement loops". A minimum of only two arc-shaped steel fibers are needed to form an enclosed area to control the development of cracks, whereas a hooked-end steel fiber requires three or more fibers. Consequently, the cracks can be closed more effectively to slow down the propagation rate. This increases the time and energy required to damage the concrete.

The combined action of the above mechanisms can effectively suppress crack development, and hence significantly improve the compression performance of SIFCON. Fig. 7 compares the action mechanisms of hooked-end steel fibers and arc-shaped steel fibers. Fig. 8 shows the "fiber cross-lock" which can be visually observed on the crack surface of an A-SIFCON specimen.

3.3 Dynamic compressive properties

The test data of strain rate, dynamic compressive strength, dynamic increase factor (DIF), and strain at peak stress of the brittle matrix and A-SIFCON specimens under dynamic load are listed in Table 4.

3.3.1 Dynamic failure patterns

Fig. 9 shows the failure patterns of brittle matrix at various strain rates. The brittle matrix tended to become more fragmented when the strain rate was high, because more cracks have to form to dissipate the energy. Increasing strain rates resulted in more severe damage to the brittle matrix.

Fig. 10 shows the failure patterns of A-SIFCON at various strain rates. A-SIFCON remained intact and only a few fragments became detached from the surface of the specimen at relatively low strain rates (e.g., 28.0 s^{-1}). In contrast, at medium strain rates (e.g., 98.2 s^{-1}), the surface of A-SIFCON was broken and mortar spalling occurred, accompanied by the detachment of a small amount of arc-shaped steel fibers. Finally, at relatively high strain rates (e.g., 164.1 s^{-1}), many arc-shaped steel fibers in the A-SIFCON were exposed, and the mortar at the side surface had completely peeled off. Obviously, the degree of damage to A-SIFCON increased with the strain rate.

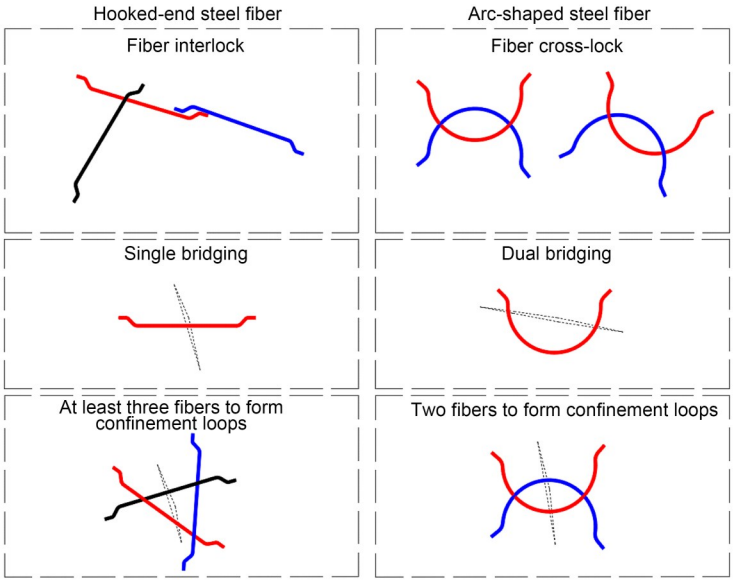

Fig. 7 Comparison of the crack-resisting mechanisms of hooked-end steel fibers and arc-shaped steel fibers

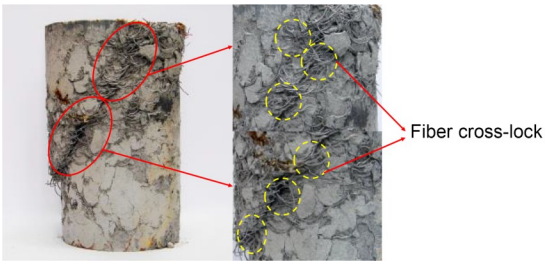

Fig. 8 "Fiber cross-lock" at the crack surface of an A-SIFCON specimen

Nevertheless, the damage was not explosive and the specimens did not shatter.

The failure patterns of conventional SFRC at relatively high strain rates tend to be more fragmented (Li et al., 2016; Liao et al., 2020; Yu et al., 2021). Given the less fragmented failure pattern of A-SIFCON specimens, we deduced that the dynamic toughness and energy absorption capacity of A-SIFCON at similar strain rates are higher than those of SFRC. This might be due to the significantly higher fiber volume fractions of A-SIFCON compared with other fiber reinforced concretes in general. When subject to impact load, the large number of arc-shaped steel fibers interconnected with each other in A-SIFCON could effectively limit the damage to the cementitious matrix.

3.3.2 Dynamic compressive stress-strain curves

Fig. 11 shows the dynamic compressive stress-strain curves of brittle matrix and A-SIFCON at various strain rates. The stress-strain curves of brittle matrix at three strain rates showed a consistent overall trend, with ascending and then descending stages (Fig. 11a). Firstly, the stress increased linearly with strain in the ascending part of the curve. This was attributed to the elasticity of the matrix in the initial stage. After the peak stress was reached, it decreased rapidly with further increase in strain.

The A-SIFCON showed the same trend in the ascending stage of the curve for different strain rates, where the stress increased linearly with the strain (Fig. 11b). However, there were two distinct kinds of descending curves. At relatively low strain rates, the stress dropped rapidly. This might have been due to unstable air pressure in the SHPB leading to premature unloading of the specimen before the actual peak stress was reached. This explanation was supported by the lack of obvious damage to the specimens under low strain rates. Therefore, the curve corresponding to low strain rates might not be the real stress-strain curve, and the measured peak stress might be lower than the actual strength value. At higher strain rates, the post-peak stress decreased slowly with increasing strain, which reflected the typical strain-softening behavior of fiber reinforced cementitious materials.

Fig. 12 shows plots of the dynamic compressive stress-strain curves of brittle matrix and A-SIFCON specimens at comparable strain rates. Comparing the peak responses, in the range of medium strain rate around 100 s^{-1}, the dynamic compressive strength of

Table 4 Dynamic compressive properties of brittle matrix and A-SIFCON

Type	Strain rate (s^{-1})	Dynamic compressive strength (MPa)	Strain at peak stress (%)	Static compressive strength (MPa)	DIF
Brittle matrix	75.7	110.8	0.44	95.6	1.16
	89.0	106.9	0.46	95.6	1.12
	109.4	138.1	0.14	95.6	1.39
	115.2	143.3	0.09	95.6	1.49
	126.7	131.4	0.21	95.6	1.37
	137.7	132.8	0.70	95.6	1.39
	168.1	146.4	0.39	95.6	1.53
	168.5	146.7	0.71	95.6	1.53
	190.4	160.6	0.27	95.6	1.68
A-SIFCON	22.7	179.0	0.77	178.0	1.00
	28.0	169.3	0.95	178.0	0.95
	30.5	169.8	1.00	178.0	0.95
	96.6	191.7	0.99	178.0	1.08
	98.2	185.6	1.19	178.0	1.04
	115.0	181.5	0.94	178.0	1.02
	164.1	194.7	1.28	178.0	1.09
	183.0	176.6	0.90	178.0	0.99
	186.8	189.0	0.70	178.0	1.06

Fig. 9 Failure patterns of brittle matrix specimens at various strain rates

Fig. 10 Failure patterns of A-SIFCON specimens at various strain rates

A-SIFCON was 34.4% higher than that of the brittle matrix, while in the range of higher strain rate around 165 s^{-1}, the dynamic compressive strength of A-SIFCON was 32.7% higher than that of the brittle matrix. This could be attributed to the presence of arc-shaped steel fibers which improved the compressive strength of SIFCON. Moreover, the curves of A-SIFCON specimens showed substantial post-peak resistance not found in the stress-strain response of brittle matrix specimens.

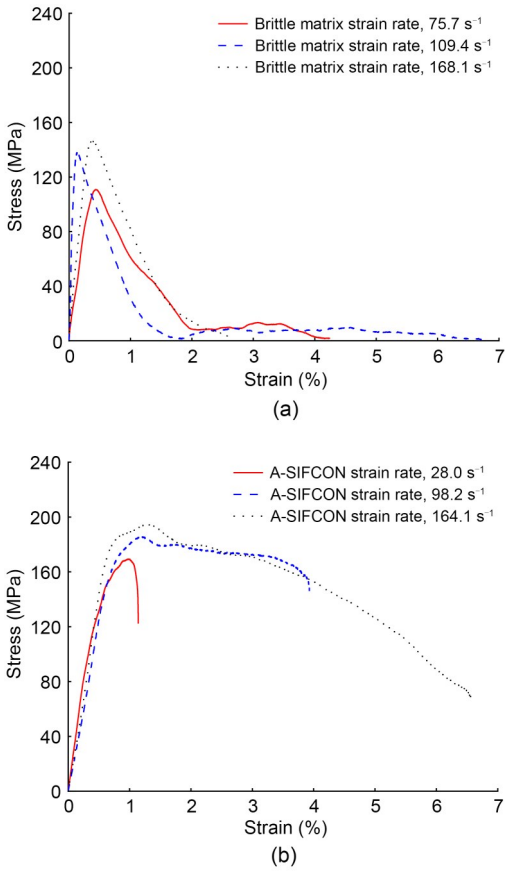

Fig. 11 Dynamic compressive stress-strain curves at various strain rates: (a) brittle matrix; (b) A-SIFCON

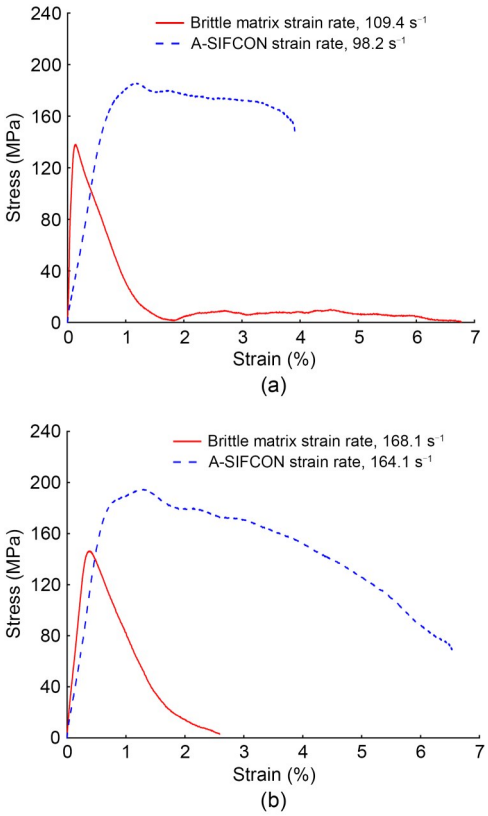

Fig. 12 Dynamic compressive stress-strain curves at comparable strain rates: (a) strain rate around 100 s^{-1}; (b) strain rate around 165 s^{-1}

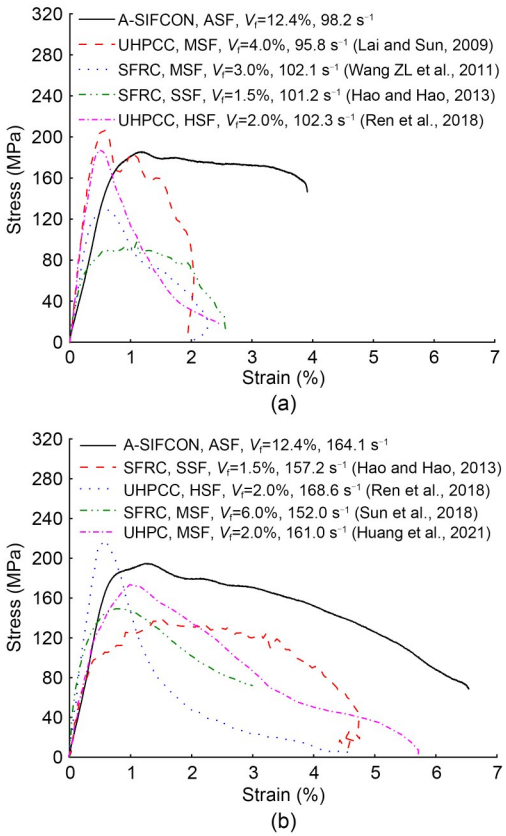

Fig. 13 Dynamic compressive stress-strain curves of different concretes at comparable strain rates: (a) strain rate around 100 s^{-1}; (b) strain rate around 165 s^{-1}. ASF: arc-shaped steel fiber; MSF: micro steel fiber; SSF: spiral steel fiber; HSF: hooked-end steel fiber; UHPCC: ultra-high performance cementitious composites; UHPC: ultra-high performance concrete

Furthermore, Fig. 13 shows a comparison of dynamic compressive stress-strain curves between the A-SIFCON and other concretes reported in the literature (Lai and Sun, 2009; Wang ZL et al., 2011; Hao and Hao, 2013; Ren et al., 2018; Sun et al., 2018; Huang et al., 2021) at comparable strain rates. The A-SIFCON in this study had both higher dynamic compressive strength and greater deformation capability. This can be explained by the new mechanisms brought about by the use of arc-shaped steel fibers enhancing the mechanical properties of SIFCON, as described in detail in Section 3.2.

3.3.3 Dynamic compressive strength

Fig. 14 shows the dynamic compressive strength of the brittle matrix and the A-SIFCON specimens under various strain rates. The dynamic compressive strength of the brittle matrix increased markedly as the strain rate increased, revealing a noticeable strain rate enhancement effect. As the strain rate increased from 75.7 to 190.4 s^{-1}, the dynamic compressive strength

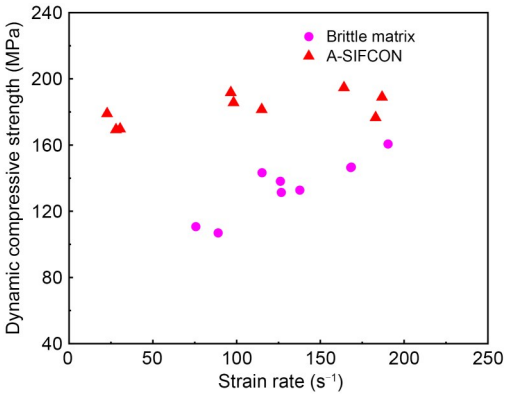

Fig. 14 Plot of dynamic compressive strength of brittle matrix and A-SIFCON versus strain rate

increased by 44.9%. This shows that the brittle matrix is a material that is sensitive to strain rate.

In contrast, the dynamic compressive strength of A-SIFCON increased only slightly with increasing

strain rate. The dynamic compressive strength increased by only 11.6% as the strain rate increased from 28.0 to 186.8 s^{-1}. Therefore, the strain rate enhancement effect of A-SIFCON is less significant than that of the brittle matrix. In other words, A-SIFCON is a material that is less sensitive to strain rate than brittle matrix.

The DIF is an essential parameter used to describe the relationship between the compressive strength of materials and the strain rate. This concept has been proposed for the design and analysis of concrete structures subject to dynamic load in engineering practice (U.S. Army Corps of Engineers NFEC, Air Force Civil Engineer Support Agency, 2008). Based on the ratio of dynamic to quasi-static compressive strength, the DIF is calculated by

$$\mathrm{DIF}=\frac{f_{\mathrm{c}}}{f_{\mathrm{cs}}}, \tag{2}$$

where f_{cs} is the quasi-static compressive strength and f_{c} is the dynamic compressive strength of a test specimen.

The DIF values for the brittle matrix and A-SIFCON specimens are plotted against the strain rate in Fig. 15. The DIF values for the brittle matrix are generally higher than those for A-SIFCON specimens. This reflects a proportionately smaller increase in f_{c} relative to f_{cs} for A-SIFCON than for the brittle matrix. This may be because of both a size effect and the stress wave propagation velocity. Regarding the size effect, the dynamic compression specimen was prepared by cutting the static compression specimen and was therefore smaller in size. For the static compression specimen, the interconnection between the arc-shaped steel fibers of A-SIFCON contributed to the enhancement of the quasi-static compressive strength. Conversely, the small size of the dynamic compression specimen limited the effectiveness of the hooking mechanism of arc-shaped steel fibers (note that the specimen height of 34 mm was only 1.9 times the span and 3.1 times the rise of the arc-shaped steel fibers). Moreover, the arc-shaped steel fibers may have been partially distorted or damaged during the specimen cutting process, thereby weakening the interlinking between the fibers. Therefore, the improvement of dynamic compressive strength of the A-SIFCON specimens would be less significant. To this end, further research in designing a better dynamic compression test method to fully reflect the contributions of the arc-shaped steel fibers is recommended. Regarding the stress wave propagation velocity, considering the case of A-SIFCON, the existence of steel fibers limits crack development. This would slow down the crack propagation velocity. Moreover, the high-volume content of steel fibers would facilitate stress transfer. Hence, the stress wave would propagate faster than the crack, especially at high strain rates. The lower crack velocity would render a lower proportional improvement in dynamic compressive strength of A-SIFCON specimens, and hence lower DIF values than the brittle matrix specimens (Wang SS et al., 2011).

The Fib Model Code 2010 (2013) provides a formulation to model concrete dynamic compression performance based on strain rate, as follows:

$$\mathrm{DIF}=\frac{f_{\mathrm{c}}}{f_{\mathrm{cs}}}=\begin{cases}\left(\dfrac{\dot{\varepsilon}}{\dot{\varepsilon}_{\mathrm{s}}}\right)^{0.014}, & \dot{\varepsilon}\leqslant 30\ \mathrm{s}^{-1},\\ 0.012\left(\dfrac{\dot{\varepsilon}}{\dot{\varepsilon}_{\mathrm{s}}}\right)^{\frac{1}{3}}, & \dot{\varepsilon}>30\ \mathrm{s}^{-1},\end{cases} \tag{3}$$

where f_{c} is the dynamic compressive strength at strain rate $\dot{\varepsilon}$, which falls within the range from 3×10^{-5} to 300 s^{-1}; f_{cs} is the quasi-static compressive strength at quasi-static strain rate $\dot{\varepsilon}_{\mathrm{s}}$. $\dot{\varepsilon}_{\mathrm{s}}$ is taken as 3×10^{-5} s^{-1}.

Also shown in Fig. 15 is the DIF versus strain rate for the Fib Model Code 2010 formulation. The DIF values for the two materials are overestimated by the model in Fib Model Code 2010. Therefore, an alternative model needs to be developed to predict the DIF of brittle matrix and A-SIFCON, rather than directly adopting the formula in the Fib Model Code 2010.

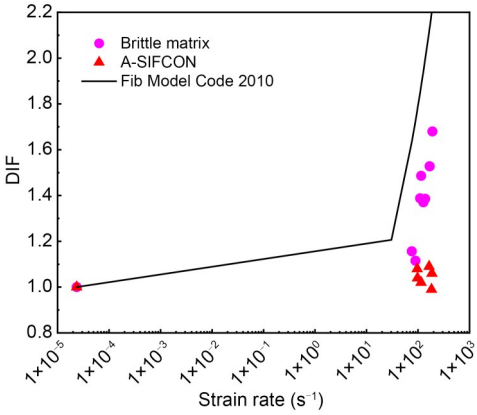

Fig. 15 Variation of DIF with strain rate of the brittle matrix and the A-SIFCON specimens

3.3.4 Dynamic toughness

The energy absorption is an essential index to evaluate the dynamic mechanical performance of materials. It is usually referred to as the material "toughness", which nominally is measured by determining the area under the stress-strain curve (Gopalaratnam et al., 1991). According to the stress-strain curves of the brittle matrix and A-SIFCON, Fig. 16 plots the corresponding average dynamic toughness with regard to the strain at peak stress versus the strain rate. According to the results, the dynamic toughness of A-SIFCON increases with the strain rate, while that of the brittle matrix decreases first and subsequently increases with the strain rate. The maximum dynamic toughness was 1.50 MJ/m^3 for A-SIFCON and 0.44 MJ/m^3 for the brittle matrix. Within ranges of comparable strain rates (96.6–115.0 s^{-1} to 109.4–137.7 s^{-1} and 164.1–186.8 s^{-1} to 168.1–190.4 s^{-1}), the dynamic toughness of the A-SIFCON was 10.08 times and 3.41 times that of the brittle matrix, respectively. The underlying reason is that the brittle matrix had lower resistance to crack formation and propagation, and hence cracked more rapidly under the dynamic load. In contrast, the arc-shaped steel fibers would be effective in resisting crack formation and propagation. The dynamic toughness of the A-SIFCON specimens was higher as a result of the arc-shaped steel fibers dissipating a significant amount of energy.

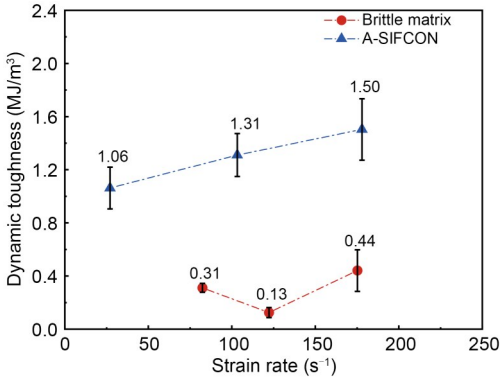

Fig. 16 Plot of dynamic toughness of brittle matrix and A-SIFCON versus strain rate

4 Conclusions

Arc-shaped steel fibers were used to produce a new class of SIFCON. To investigate the advantages of arc-shaped steel fibers over ordinary hooked-end steel fibers, the quasi-static compressive properties of SIFCON incorporating each type of steel fiber were studied experimentally. A SHPB was also used to investigate the dynamic compressive behavior of the cementitious matrix phase of SIFCON (brittle matrix) and SIFCON incorporating arc-shaped steel fibers. The crack-resisting mechanisms of hooked-end steel fibers and arc-shaped steel fibers, as well as the failure patterns, dynamic compressive strength, stress-strain curves, DIF, and dynamic toughness of brittle matrix and SIFCON were discussed. The following primary conclusions may be drawn from the findings of this research:

1. The quasi-static compressive performance of SIFCON can be significantly improved by using arc-shaped steel fibers in lieu of ordinary hooked-end steel fibers at a similar fiber volume fraction and the same fiber aspect ratio.

2. The "fiber cross-lock" mechanism, "dual bridging" over crack surfaces, and formation of "confinement loops" by a minimum of two fibers for arc-shaped steel fibers in SIFCON can effectively improve the quasi-static compression properties. Also, note that in the dynamic compression test, the smaller size of the specimen and the cutting process led to a potential diminishing of the "fiber cross-lock" mechanism, which might have limited the improvement of dynamic compression properties. We recommend further research to adopt a better dynamic compression test method to fully reflect the contributions of the arc-shaped steel fibers.

3. Both the brittle matrix and arc-shaped steel fiber SIFCON are strain rate-sensitive materials, in which the dynamic compressive strength, DIF, and dynamic toughness increase with the strain rate. From the test results, the DIF of the brittle matrix and arc-shaped steel fiber SIFCON were overestimated by the formulation in Fib Model Code 2010 at high strain rates. Therefore, it is necessary to develop an alternative DIF model for brittle matrix and arc-shaped steel fiber SIFCON material.

4. Compared with other fiber reinforced concretes, the arc-shaped steel fiber SIFCON had greater deformation and energy absorption capabilities at similar strain rates. Evidently, SIFCON incorporating arc-shaped steel fibers has desirable impact load resistance for structural applications.

Acknowledgments

This work is supported by the National Natural Science Foundation of China (Nos. 52278281, 51978624, and 51908505).

Author contributions

Hedong LI, P.L. NG, and Christopher K.Y. LEUNG designed the research. Hedong LI and Yabiao LI processed the corresponding data. Yabiao LI wrote the first draft of the manuscript. Yunfeng PAN, Xin ZHAO, P.L. NG, and Christopher K.Y. LEUNG helped to organize the manuscript. Yabiao LI revised and edited the final version.

Conflict of interest

Hedong LI, Yabiao LI, Yunfeng PAN, P.L. NG, Christopher K.Y. LEUNG, and Xin ZHAO declare that they have no conflict of interest.

References

Abirami T, Loganaganandan M, Murali G, et al., 2019. Experimental research on impact response of novel steel fibrous concretes under falling mass impact. *Construction and Building Materials*, 222:447-457. https://doi.org/10.1016/j.conbuildmat.2019.06.175

Bischoff PH, Perry SH, 1991. Compressive behaviour of concrete at high strain rates. *Materials and Structures*, 24(6): 425-450. https://doi.org/10.1007/BF02472016

Chu SH, 2019. Effect of paste volume on fresh and hardened properties of concrete. *Construction and Building Materials*, 218:284-294. https://doi.org/10.1016/j.conbuildmat.2019.05.131

Chu SH, 2021. Development of infilled cementitious composites (ICC). *Composite Structures*, 267:113885. https://doi.org/10.1016/j.compstruct.2021.113885

Chun PJ, Lee SH, Cho SH, et al., 2013. Experimental study on blast resistance of sifcon. *Journal of Advanced Concrete Technology*, 11(4):144-150. https://doi.org/10.3151/jact.11.144

Drdlová M, Řídký R, Čechmánek R, 2016. Influence of fibre type and fibre volume fraction on dynamic properties of slurry infiltrated fibre concrete. *Materials Science Forum*, 865:135-140. https://doi.org/10.4028/www.scientific.net/MSF.865.135

Drdlová M, Bibora P, Čechmánek R, 2018a. Blast resistance of slurry infiltrated fibre concrete with hybrid fibre reinforcement. *IOP Conference Series: Materials Science and Engineering*, 379:012024. https://doi.org/10.1088/1757-899x/379/1/012024

Drdlová M, Sviták O, Bibora P, et al., 2018b. Blast resistance of slurry infiltrated fibre concrete with waste steel fibres from tires. *MATEC Web of Conferences*, 149:01060. https://doi.org/10.1051/matecconf/201814901060

Elavarasi D, Saravana Raja Mohan K, 2018. On low-velocity impact response of SIFCON slabs under drop hammer impact loading. *Construction and Building Materials*, 160:127-135. https://doi.org/10.1016/j.conbuildmat.2017.11.013

Elnono MA, Salem HM, Farahat AM, et al., 2009. Use of slurry infiltrated fiber concrete in reinforced concrete corner connections subjected to opening moments. *Journal of Advanced Concrete Technology*, 7(1):51-59. https://doi.org/10.3151/jact.7.51

Fib Model Code 2010, 2013. Fib Model Code for Concrete Structures 2010. Ernst & Sohn, a Wiley Brand, Lausanne, Switzerland.

Gopalaratnam VS, Shah SP, Batson G, et al., 1991. Fracture toughness of fiber reinforced concrete. *Materials Journal*, 88(4):339-353. https://doi.org/10.14359/1840

Gulkan P, Korucu H, 2011. High-velocity impact of large caliber tungsten projectiles on ordinary Portland and calcium aluminate cement based HPSFRC and SIFCON slabs–part II: numerical simulation and validation. *Structural Engineering and Mechanics*, 40(5):617-636. https://doi.org/10.12989/sem.2011.40.5.617

Hao Y, Hao H, 2013. Dynamic compressive behaviour of spiral steel fibre reinforced concrete in split Hopkinson pressure bar tests. *Construction and Building Materials*, 48:521-532. https://doi.org/10.1016/j.conbuildmat.2013.07.022

Homrich JR, Naaman AE, 1987. Stress-Strain Properties of Sifcon in Compression. American Concrete Institute, p.283-304.

Huang HH, Gao XJ, Khayat KH, 2021. Contribution of fiber orientation to enhancing dynamic properties of UHPC under impact loading. *Cement and Concrete Composites*, 121:104108. https://doi.org/10.1016/j.cemconcomp.2021.104108

Ipek M, Aksu M, 2019. The effect of different types of fiber on flexure strength and fracture toughness in SIFCON. *Construction and Building Materials*, 214:207-218. https://doi.org/10.1016/j.conbuildmat.2019.04.055

Kar DRL, 1984. Properties, applications: slurry infiltrated fiber concrete (SIFCON). *Concrete International*, 6(12): 44-47.

Khamees SS, Kadhum MM, Alwash NA, 2020. Effects of steel fibers geometry on the mechanical properties of SIFCON concrete. *Civil Engineering Journal*, 6(1):21-33. https://doi.org/10.28991/cej-2020-03091450

Kim JJ, Yoo DY, Banthia N, 2021. Benefits of curvilinear straight steel fibers on the rate-dependent pullout resistance of ultra-high-performance concrete. *Cement and Concrete Composites*, 118:103965. https://doi.org/10.1016/j.cemconcomp.2021.103965

Kim S, Han S, Park C, et al., 2020. Compressive behavior characteristics of high-performance slurry-infiltrated fiber-reinforced cementitious composites (SIFRCCs) under uniaxial compressive stress. *Materials*, 13(1):159. https://doi.org/10.3390/ma13010159

Kim SK, Choi JH, 2006. Compressive and tensile strength properties of slurry infiltrated fiber concrete. *Journal of the Korea Concrete Institute*, 18(5):703-708. https://doi.org/10.4334/JKCI.2006.18.5.703

Kolias S, Georgiou C, 2005. The effect of paste volume and

of water content on the strength and water absorption of concrete. *Cement and Concrete Composites*, 27(2):211-216. https://doi.org/10.1016/j.cemconcomp.2004.02.009

Kolsky H, 1949. An investigation of the mechanical properties of materials at very high rates of loading. *Proceedings of the Physical Society. Section B*, 62(11):676-700. https://doi.org/10.1088/0370-1301/62/11/302

Kong YK, Kurumisawa K, Chu SH, 2022. Infilled cementitious composites (ICC)–a comparative life cycle assessment with UHPC. *Journal of Cleaner Production*, 377: 134051. https://doi.org/10.1016/j.jclepro.2022.134051

Korucu H, Gulkan P, 2011. High-velocity impact of large caliber tungsten projectiles on ordinary Portland and calcium aluminate cement based HPSFRC and SIFCON slabs–part I: experimental investigations. *Structural Engineering and Mechanics*, 40(5):595-616. https://doi.org/10.12989/sem.2011.40.5.595

Lai JZ, Sun W, 2009. Dynamic behaviour and visco-elastic damage model of ultra-high performance cementitious composite. *Cement and Concrete Research*, 39(11):1044-1051. https://doi.org/10.1016/j.cemconres.2009.07.012

Lankard DR, 1984. Slurry infiltrated fiber concrete (SIFCON): properties and applications. *MRS Online Proceedings Library*, 42(1):277-286. https://doi.org/10.1557/PROC-42-277

Lankard DR, 1985. Preparation, properties and applications of concrete-based composites containing 5% to 20% steel fiber. Steel Fiber Concrete, US-Sweden Joint Seminar, p.199-217.

Li QH, Zhao X, Xu SL, et al., 2016. Influence of steel fiber on dynamic compressive behavior of hybrid fiber ultra high toughness cementitious composites at different strain rates. *Construction and Building Materials*, 125:490-500. https://doi.org/10.1016/j.conbuildmat.2016.08.066

Liao L, Zhao J, Zhang F, et al., 2020. Experimental study on compressive properties of SFRC under high strain rate with different fiber content and aspect ratio. *Construction and Building Materials*, 261:119906. https://doi.org/10.1016/j.conbuildmat.2020.119906

Manolia AA, Shakir AS, Qais JF, 2018. The effect of fiber and mortar type on the freezing and thawing resistance of slurry infiltrated fiber concrete (SIFCON). *IOP Conference Series: Materials Science and Engineering*, 454: 012142. https://doi.org/10.1088/1757-899x/454/1/012142

Morishima S, Yamaguchi M, Shibuya S, et al., 2020. Effects of fiber type on blast resistance of slurry-infiltrated fiber concrete under contact detonation. *Journal of Advanced Concrete Technology*, 18(4):157-167. https://doi.org/10.3151/jact.18.157

Naaman AE, Otter D, Najm H, 1992. Elastic modulus of SIFCON in tension and compression. *Materials Journal*, 88(6):603-613. https://doi.org/10.14359/1197

Naji HF, Hussein MJ, Farsangi EN, 2021. Mechanical properties of SIFCON with variation steel fiber ratio and nano kaolin. *Journal of Mechanical Engineering Research and Developments*, 44(2):363-370.

Ogawa K, 1984. Impact-tension compression test by using a split-Hopkinson bar. *Experimental Mechanics*, 24(2):81-86. https://doi.org/10.1007/BF02324987

Persson PA, Holmberg R, Lee J, 1993. Rock Blasting and Explosives Engineering. CRC Press, Boca Raton, USA, p.560.

Piasta W, Zarzycki B, 2017. The effect of cement paste volume and w/c ratio on shrinkage strain, water absorption and compressive strength of high performance concrete. *Construction and Building Materials*, 140:395-402. https://doi.org/10.1016/j.conbuildmat.2017.02.033

Rao HS, Ghorpade VG, Ramana NV, et al., 2010. Response of SIFCON two-way slabs under impact loading. *International Journal of Impact Engineering*, 37(4):452-458. https://doi.org/10.1016/j.ijimpeng.2009.06.003

Reinhardt HW, Naaman AE, 1992. International workshop—high performance fibre reinforced cement composites. *Materials and Structures*, 25(1):60-62. https://doi.org/10.1007/BF02472215

Ren GM, Wu H, Fang Q, et al., 2018. Effects of steel fiber content and type on dynamic compressive mechanical properties of UHPCC. *Construction and Building Materials*, 164:29-43. https://doi.org/10.1016/j.conbuildmat.2017.12.203

Renuka J, Rajasekhar K, 2021. Performance of slurry infiltrated fibrous concrete–a comprehensive review. *Journal of Engineering Science and Technology Review*, 14(5):163-172. https://doi.org/10.25103/jestr.145.19

Ross CA, Thompson PY, Tedesco JW, 1989. Split-Hopkinson pressure-bar tests on concrete and mortar in tension and compression. *Materials Journal*, 86(5):475-481. https://doi.org/10.14359/2065

Schneider B, 1992. Development of SIFCON through applications. *In*: Reinhardt HW, Naaman AE (Eds.), High Performance Fiber Reinforced Cement Composites. RILEM, p.177-194. https://doi.org/10.1097/01.CCM.0000178288.70057.47

Shi XJ, Park P, Rew Y, et al., 2020. Constitutive behaviors of steel fiber reinforced concrete under uniaxial compression and tension. *Construction and Building Materials*, 233:117316. https://doi.org/10.1016/j.conbuildmat.2019.117316

Soylu N, Bingöl AF, 2019. Research on effect of the quantity and aspect ratio of steel fibers on compressive and flexural strength of sifcon. *Challenge Journal of Structural Mechanics*, 5(1):29-34. https://doi.org/10.20528/cjsmec.2019.01.004

Su HY, Xu JY, Ren WB, 2014. Mechanical properties of ceramic fiber-reinforced concrete under quasi-static and dynamic compression. *Materials & Design*, 57:426-434. https://doi.org/10.1016/j.matdes.2013.12.061

Sun XW, Zhao K, Li YC, et al., 2018. A study of strain-rate effect and fiber reinforcement effect on dynamic behavior of steel fiber-reinforced concrete. *Construction and Building Materials*, 158:657-669. https://doi.org/10.1016/j.conbuildmat.2017.09.093

Tuyan M, Yazıcı H, 2012. Pull-out behavior of single steel

fiber from SIFCON matrix. *Construction and Building Materials*, 35:571-577. https://doi.org/10.1016/j.conbuildmat.2012.04.110

U.S. Army Corps of Engineers NFEC, Air Force Civil Engineer Support Agency, 2008. Structures to Resist the Effects of Accidental Explosions. UFC 3-340-02, Department of Defense, USA.

Wang SS, Zhang MH, Quek ST, 2011. Effect of high strain rate loading on compressive behaviour of fibre-reinforced high-strength concrete. *Magazine of Concrete Research*, 63(11):813-827.

Wang ZL, Shi ZM, Wang JG, 2011. On the strength and toughness properties of SFRC under static-dynamic compression. *Composites Part B: Engineering*, 42(5):1285-1290.

Won JP, Lee JH, Lee SJ, 2015a. Bonding behaviour of arch-type steel fibres in a cementitious composite. *Composite Structures*, 133:117-123.

Won JP, Lee JH, Lee SJ, 2015b. Flexural behaviour of arch-type steel fibre reinforced cementitious composites. *Composite Structures*, 134:565-571.

Wu ZM, Khayat KH, Shi CJ, 2018. How do fiber shape and matrix composition affect fiber pullout behavior and flexural properties of UHPC? *Cement and Concrete Composites*, 90:193-201.

Yu QL, Zhuang WT, Shi CJ, 2021. Research progress on the dynamic compressive properties of ultra-high performance concrete under high strain rates. *Cement and Concrete Composites*, 124:104258. https://doi.org/10.1016/j.cemconcomp.2021.104258